Langmuir

Article

pubs.acs.org/Langmuir

Room-Temperature Compressive Transfer Printing of Nanowires for Nanoelectronic Devices

Won Seok Lee,[†] Jun-hyeok Choi,[‡] Inkyu Park,*[,†,§,∥] and Jihye Lee*[,‡]

[†]Department of Mechanical Engineering, [§]KI for the NanoCentury (KINC), and [∥]Mobile Sensor and IT Convergence (MOSAIC) Center, Korea Advanced Institute of Science and Technology (KAIST), Daejeon 305-701, Korea

[‡]Department of Nano Manufacturing Technology, Korea Institute of Machinery and Materials (KIMM), Daejeon 305-343, Korea

Supporting Information

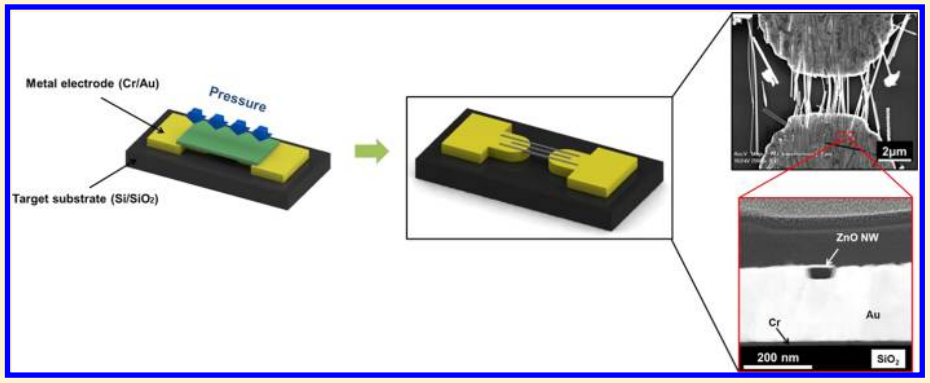

ABSTRACT: Recently, there has been a growing interest in the controlled alignment and robust bonding process of nanowires (NWs) on nanoelectronic devices. In this paper, we developed an innovative process for the fabrication of NW-based devices by room-temperature and low-pressure compressive transfer printing of NWs, in which NWs could be simultaneously aligned and bonded onto the metal electrodes. In this process, chemically synthesized NWs were first transferred and aligned on an intermediate substrate by contact printing and then finally printed onto a target substrate with mechanically soft Au electrodes, which enables the embedding of aligned NWs under low-pressure (5 bar) and room-temperature condition. The resulting contact between NW and Au electrodes exhibits Schottky behavior and high mechanical bonding strength (>567 MPa). The electrical characteristics could be converted from Schottky to Ohmic contact through thermal annealing treatment at 250 °C for 5 min due to Cr diffusion and direct Cr-ZnO contact formation. The applications of the fabricated devices as ultraviolet (UV) and gas sensors were successfully demonstrated. Furthermore, NW-based electronic devices were fabricated on a flexible substrate by using this process and showed mechanical and electrical robustness under mechanical bending conditions.

INTRODUCTION

Recently, there have been very active studies on the fabrication of nanowire (NW)-based devices by integrating chemically synthesized NWs[1−5] in device platforms for their applications such as light-emitting diodes,[6] sensors,[7−10] transistors,[11,12] lab-on-a-chip devices,[13] and power generation devices.[14,15] Various approaches such as dielectrophoresis,[16−21] magnetophoresis,[22] nanomanipulation,[23] and contact printing[24] for the alignment of NWs onto device platforms with prepatterned metal electrodes have been developed. Although NWs could be aligned onto the metal electrodes by those methods, only weak bonding is formed between the NWs and the metal electrodes based on the van der Waals force. This weak bonding can cause unstable electrical characteristics of devices and mechanical failure by thermally or mechanically driven stresses. The mechanical instability of weak NW−electrode bonding is even more critical for flexible electronic devices, in which various mechanical deformation modes (bending, twisting, and stretching) are exerted. Therefore, various approaches such as focused ion beam (FIB) induced deposition,[17] selective electrodeposition,[18,25] photolithography,[19,23] soldering,[20,22] and hot-pressing[21] have been developed to achieve mechanically and electrically robust contacts between NWs and metal electrodes. However, these bonding processes occurring after NW alignment steps cause fabrication complexity, low manufacturing throughput, and increased manufacturing and material costs. Also, previously developed bonding processes have several drawbacks as follows: The FIB deposition method has a low throughput due to serial Pt deposition process and requires high manufacturing cost because of expensive equipment. Selective electrodeposition methods cannot be applied to many semiconductor materials (ex. ZnO NWs) that react with the chemical solutions used for the electrodeposition process. Also, this method cannot be applied to the metal

Received: September 8, 2012
Revised: November 5, 2012

   dx.doi.org/10.1021/la3036133 | Langmuir XXXX, XXX, XXX−XXX

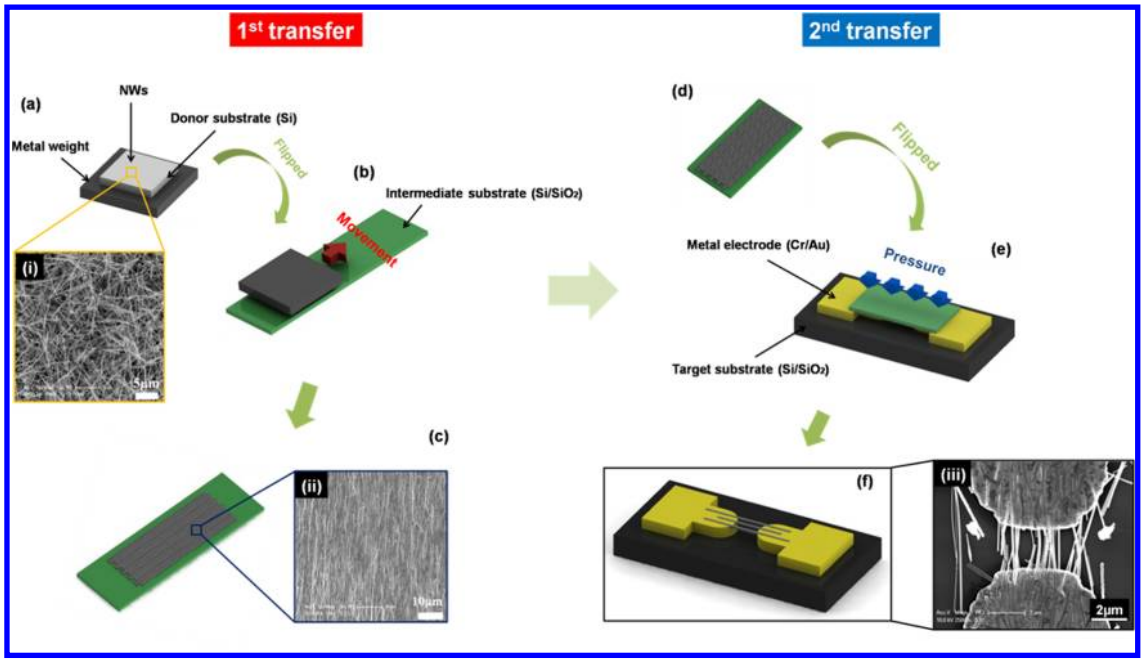

Figure 1. Process flow of room-temperature compressive transfer printing: (a) NWs on donor substrate that is attached to a metal weight; (b) transfer of the NWs from a donor substrate to an intermediate substrate by contact printing; NWs were pressed by a metal weight and moved with a constant velocity; (c) NWs aligned along the sliding direction after the first transfer step; (d–e) transfer of NWs from an intermediate substrate to a target substrate with metal electrodes; (f) completion of the NW-based device fabrication; insets (i) and (ii) are the SEM images of NWs before and after the first transfer step and (iii) is the SEM image of a NW-based device after the second transfer step.

electrodes with small gaps because metal is also deposited onto the sidewalls as well as onto the top surface of metal electrodes. In other words, small electrode gaps can be easily closed during the electrodeposition process. In the case of the photolithography method, NWs can be contaminated or damaged during the spin coating, development, or baking processes of photoresist. Also, aligned NWs can be destroyed or detached from the substrate during the lift-off process. The soldering method is limited to only specialized nanomaterials such as Sn or In–Sn-based alloy NWs for melting or softening the solder materials at low temperatures. Last, the hot-pressing method requires high-pressure and -temperature conditions (e.g., 96 bar and 180 °C).[21] Also, the device fabricated by the hot-pressing method has high specific contact resistance (e.g., 1.1×10^{-1} $\Omega \cdot cm^2$).[21]

In order to resolve these problems, the thermo-compressive transfer printing method using indium (In)-based alloys (i.e., Au–In, Cu–In alloys) with low melting temperatures was recently developed by the authors.[26] This method could simultaneously achieve both the alignment and the robust bonding of NWs onto metal electrodes by using a two-step transfer printing technique with low pressure (5 bar) and temperature (100 °C) requirements. However, In-based alloy metal electrodes have certain limitations as follows: First, In can be easily diffused into Au or Cu at temperatures above 156 °C (melting point of In), which results in various intermetallic compounds (Au_xIn_y/Cu_xIn_y). The intermetallic compounds can degrade the electrical properties of the devices by increasing the sheet resistance of metal electrodes and also by increasing the contact resistance due to high surface roughness of the metal electrodes.[27] In the case of Au–In alloy and Cu–In alloy electrodes, the average surface roughness was measured as 25 and 41 nm, respectively.[26] Another critical problem of In-based alloy electrodes is low melting temperatures as compared to common metal electrode materials (Au, Al, etc.) for the microelectronic devices. Therefore, thermal degradation of the device can easily occur and the device cannot be used for high temperature or high power applications. In order to resolve these problems, we developed a new room-temperature compressive transfer printing process by using Au electrodes instead of In-based alloy electrodes. Au is a good candidate material for metal electrodes because of its stable electrical property and resistance to oxidation in ambient conditions as well as in high temperature conditions. Also, Au has superior ductility and malleability (elongation: 68–73%), which allows the submergence of NWs into Au electrodes by a compression process at room-temperature and low-pressure conditions.

There have been processes for low-temperature solid-state welding called "cold-welding". This process has been typically used for metal-to-metal bonding with high normal or frictional loads in clean environment and surface conditions.[28] Recently, cold welding technologies for nanomaterials have been also developed. Lu et al.[29] demonstrated high-speed bonding between metal nanowires at room-temperature and low-pressure conditions. However, this study has mainly focused on the bonding phenomena between two metal nanowires in transmission electron microscopy (TEM) without further study at the device level. Another method of low-temperature internanowire bonding is the plasmonic welding developed by Garnett et al.[30] In this work, local plasmonic excitation at nanometer-scale gaps between silver nanowires enabled strong bonding between nanowires without any heating or pressure requirements. However, this method is limited only to specialized metallic nanowires such as Ag that can create strong plasmonic resonance. Our work can be distinguished from the above-mentioned cold-welding technologies since our method is for bonding between one-dimensional nanomaterials and metal electrodes, and it can be applicable to an almost unlimited range of one-dimensional nanomaterials and metal electrodes.

dx.doi.org/10.1021/la3036133 | *Langmuir* XXXX, XXX, XXX–XXX

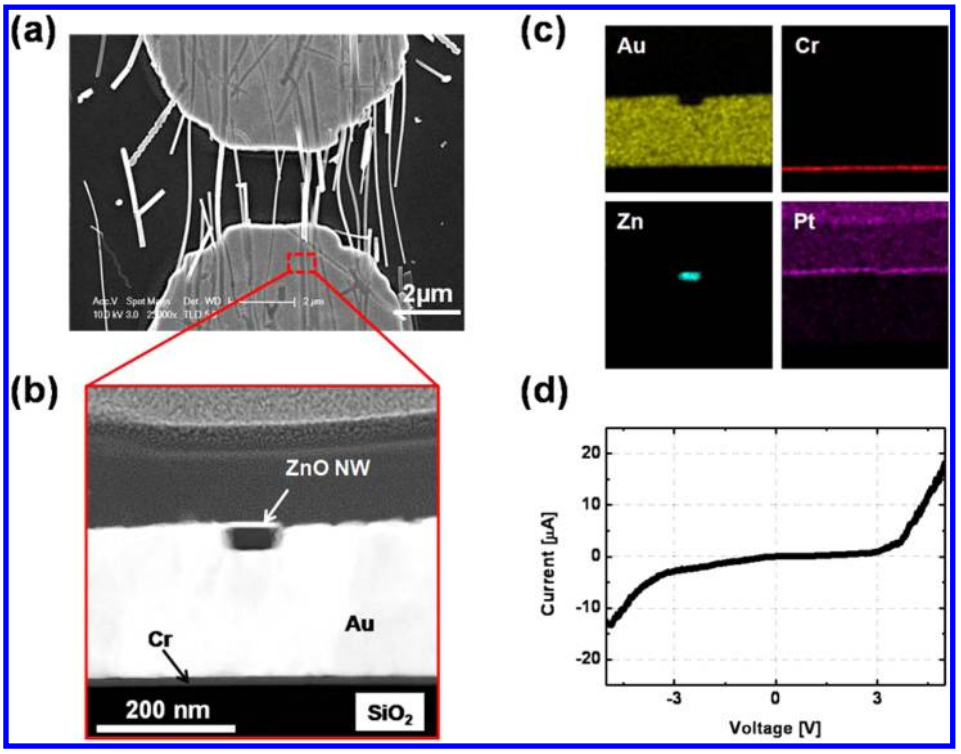

Figure 2. Microscopic analysis and electrical measurement of ZnO NW-based device fabricated by a compressive transfer printing at 5 bar and 23 °C: (a) SEM image of ZnO NWs embedded into Au electrodes and (b) TEM image and (c) EDS analysis of cross section of contact region between ZnO NW and Au electrode; (d) current−voltage (I−V) curve of the ZnO NW device.

In this paper, we have demonstrated that NWs can be embedded onto Au electrodes by a simple compressive transfer printing process at room-temperature and low-pressure conditions. We have verified that the NW-based electronic devices fabricated by room-temperature compressive transfer printing have a robust mechanical bonding strength with a Schottky contact behavior. We have also observed that the electrical characteristics can be converted from Schottky to Ohmic contact by an appropriate thermal annealing process in ambient environment.

EXPERIMENTAL SECTION

Room-Temperature Compressive Transfer Printing Process. The procedure for room-temperature compressive transfer printing is illustrated in Figure 1. The process is based on a two-step transfer technique. In the first transfer step as shown in Figure 1a−c, NWs randomly grown on a donor substrate (Si substrate) were transferred onto an intermediate substrate (Si/SiO_2 substrate) by the contact printing method[24] where normal pressure and shear forces were applied to the intermediate substrate to form an array of NWs in one direction. The donor substrate was attached to a metal weight and then was flipped over to make contact with NWs and the intermediate substrate as shown in Figure 1a,b. A normal pressure of 30 mbar was applied to the donor substrate by the metal weight. Afterward, the donor substrate was pushed with a constant velocity (15 mm/min) in one direction. In the second transfer step, a slice of intermediate substrate was pressed on a target substrate with metal electrodes at room temperature (i.e., 23 °C) and a pressure of 5 bar for 5 min (see Figure 1d,e). After detaching the intermediate substrate, the fabrication of NW device was completed as shown in Figure 1f. Furthermore, if the conversion from a Schottky to Ohmic contact was needed, the annealing process of the device was conducted for 5 min at 250 °C. To be specific, the temperature was linearly increased from 23 to 250 °C for 30 min and then maintained at 250 °C for 5 min (see Figure S1 in the Supporting Information for detailed temperature profile during the annealing process).

Preparation of NWs and Substrates. We used Sn-doped ZnO NWs grown on a Si(100) donor substrate in random directions. The details of the synthesis method are described in our previous paper.[26] As shown in the scanning electron microscopy (SEM) images (insets (i) and (ii) of Figure 1), we indicated that ZnO NWs randomly grown on the donor substrate were transferred and aligned on the intermediate substrate with high density (60−80 NWs/10 × 10 μm^2 area) and long lengths (10−20 μm). As for the target substrate, a Si substrate with a 300-nm-thick thermally oxidized SiO_2 layer was used. The source and drain electrodes composed of 10-nm-thick Cr and 200-nm-thick Au layers were fabricated by photolithography, electron beam evaporation, and lift-off process.

Characterization. Field-emission scanning electron microscopy (FE-SEM, Sirion) and Cs-corrected scanning transmission electron microscopy (Cs-corrected STEM, JEM-ARM200F) and energy-dispersive spectrometry (EDS, JEM-ARM200F) were used for analysis of the contact region between metal electrodes and NWs. A lateral force microscope (LFM, Park Systems XE-100) and semiconductor analyzer (Keithley 4200-SCS) were used for the measurement of bonding strength and electrical characteristics, respectively.

UV and Gas Sensing Experiment. For the UV sensitivity measurement, a UV lamp with a light intensity of 0.45 mW/cm^2 and a peak wavelength of λ = 365 nm was used in an ambient air, room-temperature condition. The change of current by the UV illumination was measured using a semiconductor analyzer (HP4155A, Hewlett-Packard) at a constant DC bias of 0.5 V. The gas sensitivity was measured by using a digital source meter (Keithley 2000) in the tube furnace by varying the H_2 concentrations (500−5000 ppm) with a constant flow rate of 600 sccm and at a temperature of 350 °C.

Mechanical Bending Test. The fatigue test was carried out by bending the device from $\rho = \infty$ (flat) to ρ = 10 mm constantly by 10^2−10^3 cycles using a single-axis linear motorized stage.

RESULTS AND DISCUSSION

Figure 2 shows the SEM image of ZnO NWs that were transferred from the intermediate substrate and successfully

dx.doi.org/10.1021/la3036133 | Langmuir XXXX, XXX, XXX−XXX

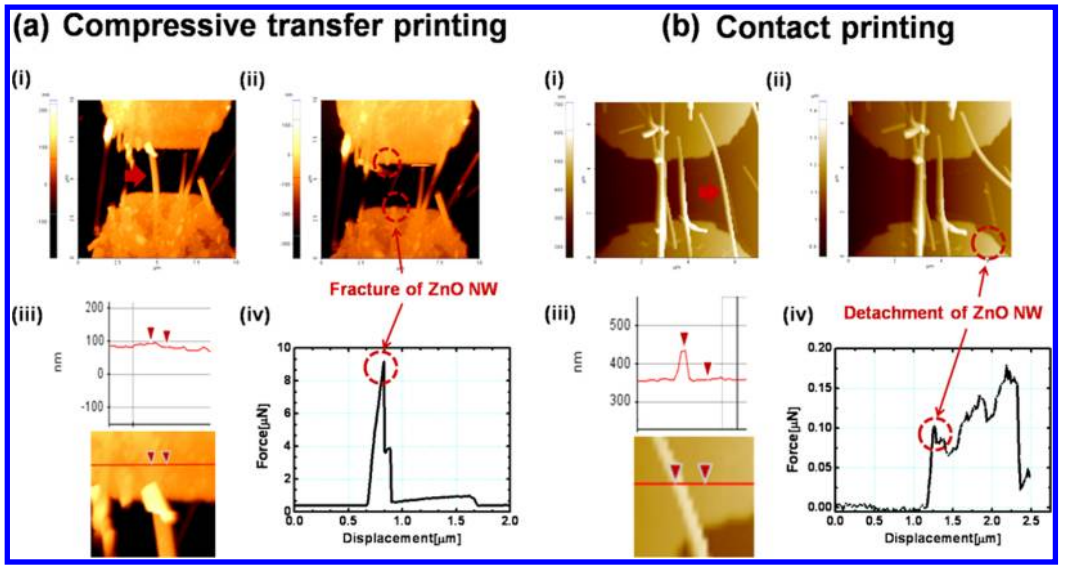

Figure 3. Comparison of mechanical bonding strength by LFM test: ZnO NW bonded on Au metal electrodes by (a) compressive transfer printing and (b) contact printing: (i) before and (ii) after applying a lateral force to the ZnO NWs in the pointed direction; (iii) line profile along the top surface of the Au electrode; (iv) plot of force versus displacement in the LFM measurement.

embedded into Au electrodes by the compression transfer printing process at 23 °C and 5 bar for 5 min. TEM-EDS mapping images in Figure 2b,c reveal that a ZnO NW was successfully embedded and contacted with Au electrodes without forming any observable voids. We have also found that the ZnO NW−Au electrode interface exhibited a Schottky contact property from the electrical measurement as shown in Figure 2d. In order to form a Schottky contact between an n-type semiconductor and metal electrodes, the work function of metal electrodes should be higher than the electron affinity of the semiconductor. Here, the contact of ZnO NW and Au electrodes formed a Schottky contact because the work function of Au is higher (5.1−5.47 eV) than the electron affinity of ZnO NW (4.2−4.35 eV).[27]

In order to analyze the submergence phenomenon of NWs into Au electrodes during the room-temperature compressive transfer printing, we conducted a numerical analysis using *ANSYS 12.0* Workbench. The von Mises yield criterion was adopted and Au was assumed to have perfectly elastic−plastic behavior based on a bilinear isotropic-hardening model to accommodate for the large deformation.[31] The degrees of freedom for the bottom and side surfaces of Si/SiO_2 substrate were constrained. A vertical displacement of 100 nm was applied at upper surface of a ZnO NW in order to simulate its submergence onto the surface of Au electrodes. The results of numerical simulation are shown in Figure S2b−d. When the ZnO NW was embedded into the Au electrodes by 100 nm, a maximum stress of 4.24 GPa and an average stress of 1.14 GPa were developed on the region of contact between the NW and Au electrodes. These values exceed the yield strength of Au (400 MPa), resulting in a permanent deformation of contact regions on the Au electrodes. Therefore, the submergence of the ZnO NW into the Au electrodes is attributed to the plastic deformation of Au electrodes by the stress above the yield strength. Figure S2d shows that the maximum plastic strain of Au electrodes was 2.79 at the contact region of the ZnO NW and Au electrodes.

We performed an LFM test[32] in order to analyze the mechanical bonding strength between ZnO NWs and Au electrodes by applying a lateral force to a single ZnO NW bonded onto the Au electrodes. We prepared two devices to compare their bonding strengths. The first device was fabricated by the room-temperature compressive transfer printing and another was fabricated by a conventional contact printing process.[24] For the second device, ZnO NWs were aligned on Au electrodes with a small normal pressure of 30 mbar while the substrate with ZnO NWs was moved with a constant velocity of 15 mm/min in one direction for 30 s. When a lateral force was applied to a ZnO NW on the target substrate as presented in Figure 3a-i,b-i, different failure phenomena occurred. In the case of the ZnO NW embedded into Au electrodes by the room-temperature compressive transfer printing, a fracture of the ZnO NW happened by a lateral force of 9 μN along the edges of Au electrodes as shown in Figure 3a-ii,iv. However, in the case of the ZnO NW positioned on the top surface of Au metal electrodes by contact printing, a detachment of the ZnO NW from Au electrode happened by a lateral force of 0.1 μN as shown in Figure 3b-ii,iv.

We calculated the bonding strengths between the ZnO NW and Au electrodes by using a numerical calculation based on *ANSYS 12.0* Workbench and experimental results of the LFM test. Figure S3 shows the results of numerical simulation for the ZnO NW device fabricated by the room-temperature compressive transfer printing with a lateral force applied. The maximum local shear stress generated at the NW−Au electrode interface was 567 MPa, the maximum local stress on the ZnO NW was 2.96 GPa, and the maximum plastic strain of Au electrodes at the contact region was 0.0011 when a lateral force of 9 μN (i.e., the force applied to the NW at the point of NW fracture in the LFM test) was applied to the center of NW. This calculation shows that mechanical bonding strength of the NW−Au electrode interface exceeds 567 MPa, which can be attributed to the embedding of NW into Au electrodes as shown in Figure 3a-iii. The mechanical embedding of NWs into the surrounding metal electrode provides a physical constraint to the displacement of NWs by external forces as well as the reinforcement of the bonding force between the NWs and electrode. For the conventional contact printing process, the maximum local shear stress at the metal electrode−NW

dx.doi.org/10.1021/la3036133 | *Langmuir* XXXX, XXX, XXX−XXX

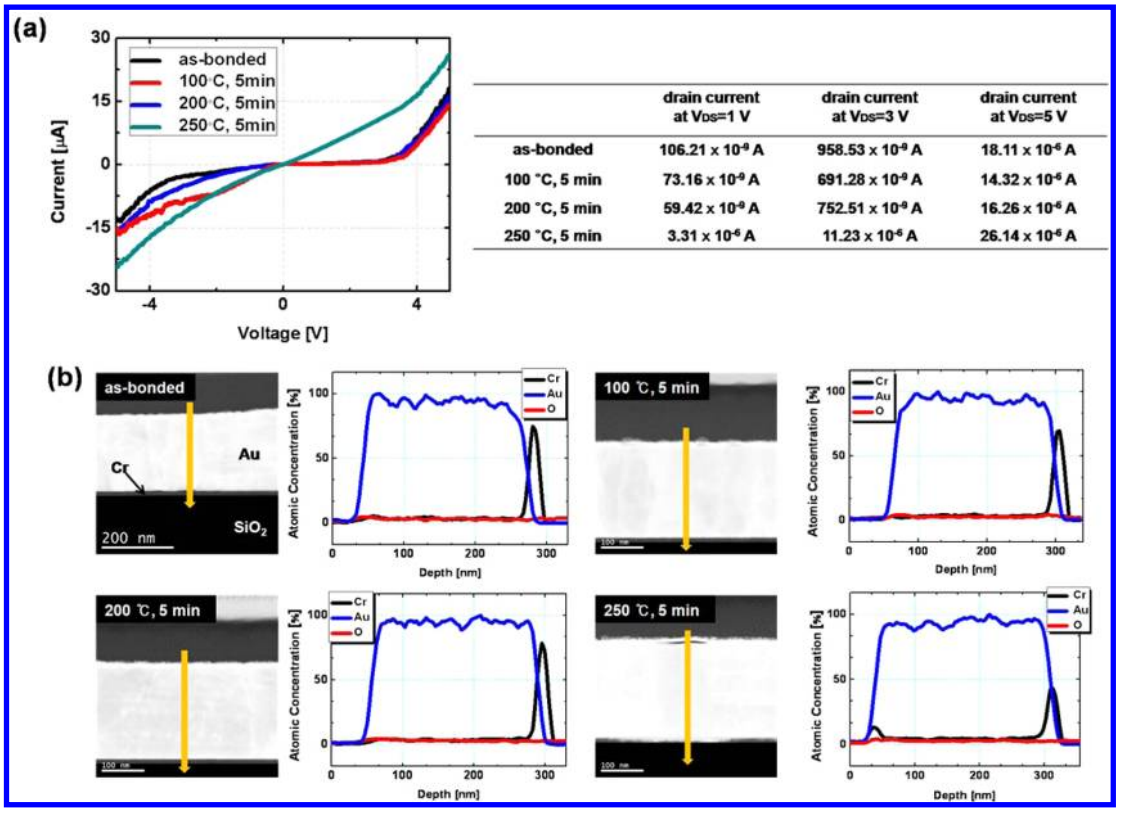

	drain current at V_{DS}=1 V	drain current at V_{DS}=3 V	drain current at V_{DS}=5 V
as-bonded	106.21 x 10^{-9} A	958.53 x 10^{-9} A	18.11 x 10^{-6} A
100 °C, 5 min	73.16 x 10^{-9} A	691.28 x 10^{-9} A	14.32 x 10^{-6} A
200 °C, 5 min	59.42 x 10^{-9} A	752.51 x 10^{-9} A	16.26 x 10^{-6} A
250 °C, 5 min	3.31 x 10^{-6} A	11.23 x 10^{-6} A	26.14 x 10^{-6} A

Figure 4. Effect of thermal annealing treatment: (a) electrical characteristics and (b) EDS line scan of cross section of metal electrodes showing that the diffusion of Cr within Au layer occurred by annealing at 250 °C for 5 min.

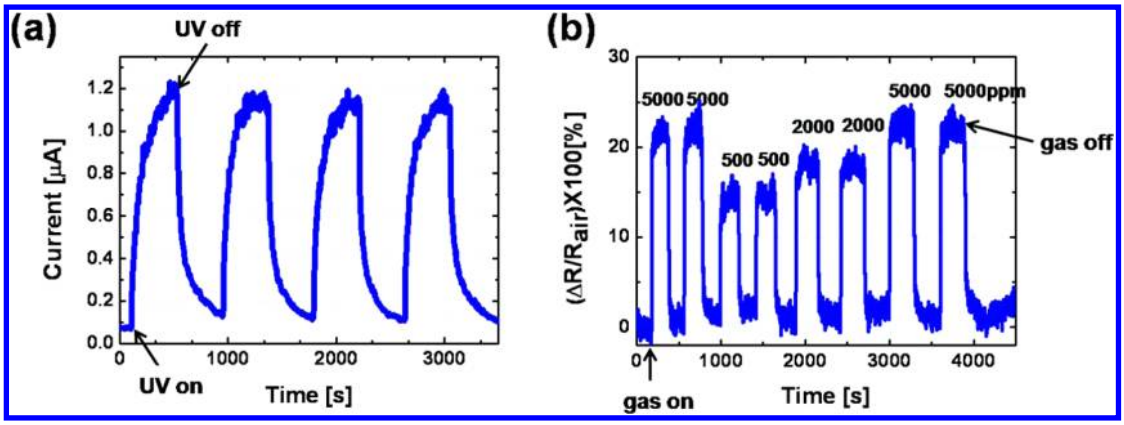

Figure 5. Application of room-temperature compressive transfer printing process to ZnO NW-based UV and gas sensors: (a) response of ZnO NW device with a Schottky contact to UV light (λ = 365 nm) in ambient air, room-temperature condition with a DC bias of 0.5 V; (b) response of ZnO NW device with Ohmic contact to various concentrations (in ppm) of H_2 gas at 350 °C and 0.5 V bias.

interface was estimated to be only 21.9 MPa by numerical analysis (see Figure S4). The maximum local stress along the ZnO NW was 0.11 GPa, and no plastic strain of metal electrodes occurred when a lateral force of 0.1 μN (i.e., force applied to the NW at the failure point in the LFM test) was applied to the center of the NW. The failure at the bonding surface (Figure 3b-ii) was caused by a low bonding strength (21.9 MPa) between the ZnO NW and Au electrode. From these results, we can conclude that the room-temperature compressive transfer printing provides a superior bonding strength (>567 MPa) compared to the conventional contact printing process (21.9 MPa). In other words, mechanically robust bonding between the NWs and metal electrodes is enabled by the room-temperature compressive transfer printing process. Here, the mechanical embedding of NWs into the surface of the metal electrode is believed to provide high bonding strengths.

Figure 4 shows the effect of thermal annealing treatment on the device characteristics. The bonding of ZnO NWs and Au electrodes formed a Schottky contact after the room-temperature compressive transfer printing process. This Schottky contact behavior was not changed by annealing at 100 °C for 5 min or at 200 °C for 5 min. However, after annealing at 250 °C for 5 min, the Schottky contact was transformed to an Ohmic contact. In order to understand this change of contact behaviors, the evolution of elemental distribution in the Au/Cr electrode during thermal annealing was measured by an EDS line scan on the cross section of the electrode as shown in

dx.doi.org/10.1021/la3036133 | Langmuir XXXX, XXX, XXX−XXX

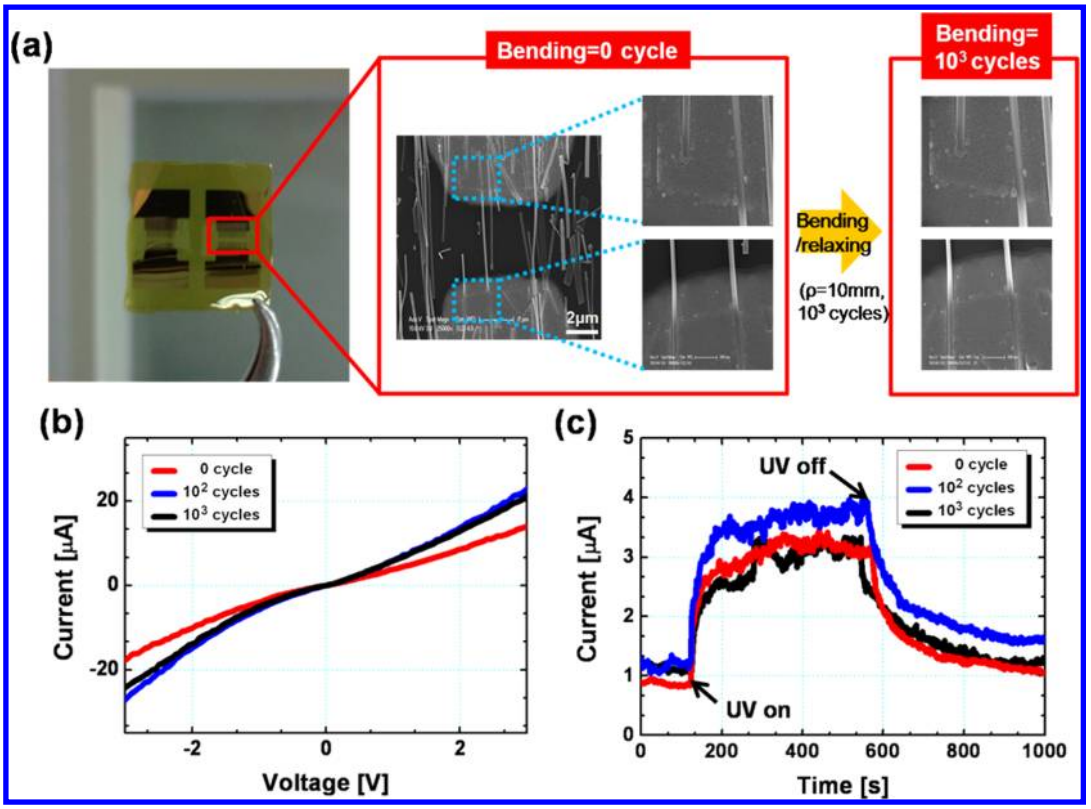

Figure 6. Mechanical bending test of flexible ZnO NW-based devices fabricated by room-temperature compressive transfer printing: (a) photography of ZnO NW-based devices on a polyimide substrate and SEM image of the ZnO NWs embedded in Au electrodes before and after 10^3 cycles of periodic bending between the curvature radii of $\rho = \infty$ and $\rho = 10$ mm. Change of (b) current−voltage characteristics and (c) responses to UV light after 10^2 and 10^3 cycles of repeated bending.

Figure 4b. In contrast to the as-bonded electrode and those annealed at 100 and 200 °C, we could find that Cr exist on the upper surface of the Au electrode after annealing at 250 °C for 5 min. Huang et al. reported that Cr can be diffused to the Au layer at 250 °C for 5 min in Cr/Au bilayer.[33] It is believed that the Cr beneath the Au layer diffused across the Au layer and approached the upper surface of Au layer.

The effect of Cr diffusion on the electrical characteristics of the ZnO NW device can be explained as follows. After annealing at 250 °C, Cr is diffused to the top surface of Au layer and forms a direct contact with a ZnO NW as shown in Figure S5. Then, Cr is changed to Cr_xO_y[34] by taking oxygen from the ZnO NW. Thus, the oxygen deficiency in ZnO NW is increased, boosting up the free electron density. As a result, the resistivity of the ZnO NW is decreased and the Schottky barrier between the ZnO NW and the metal electrodes becomes reduced. The reduced barrier enhances the electron tunneling between the ZnO NW and the metal electrodes. As a consequence, the Schottky contact is transformed to an Ohmic contact at the interface between ZnO NW and Au electrode.

The application of ZnO NW devices as UV and gas sensors was demonstrated as shown in Figure 5. As for the UV sensing results, the device with a Schottky contact showed an average on/off current ratio of 12 and time constant of 50 s by UV illumination as shown in Figure 5a. The mechanism of photodetection is known as the change of the resistivity of ZnO NW due to generated free electrons when the ZnO NW is exposed to the UV light.[35] Also, the electrons and holes are quickly generated at the Schottky contact interface by UV illumination. The generated holes induce desorption of oxygen at the Schottky barrier, which reduces the height of the Schottky barrier.[36] Therefore, the synergetic effect of reduced Schottky barrier height and increased free electron density by UV illumination enables a significant increase of electrical current through the Schottky contact device. Gas sensing performance of the ZnO NW device with an Ohmic contact is shown in Figure 5b. This device presented the decrease of electrical resistance by 13%, 18%, and 24% to 500, 2000, and 5000 ppm of H_2 concentrations, respectively. The response and recovery times were 11 and 9 s, respectively, for 500 ppm of H_2 gas. The mechanism of H_2 gas sensing can be explained as follows. In ambient environment, oxygen molecules are adsorbed on the surface of ZnO NW, and produce negatively charged oxygen ions (O^{2-}) by capturing electrons from the ZnO NW. This results in the reduction of free electrons and the generation of depletion region at the surface. When the ZnO NW is exposed to H_2 gas, the H_2 molecules react with oxygen ions on the surface of ZnO NW and produce H_2O molecules. As a result, oxygen ions are removed from the surface of the ZnO NW and the electrons are released back to the ZnO NW, resulting in the decrease of electrical resistance.[37] From the results of both UV and gas sensing applications, we believe that the devices fabricated by the room-temperature compressive transfer printing of ZnO NWs onto Au electrodes can be widely applicable to a variety of electronic devices.

Since the room-temperature compressive transfer printing uses a low-temperature (23 °C) and low-pressure (5 bar) condition, it can be applied for the fabrication of NW-based devices on flexible plastic substrates. ZnO NW devices on a

dx.doi.org/10.1021/la3036133 | *Langmuir* XXXX, XXX, XXX−XXX

flexible polyimide substrate were fabricated by room-temperature compressive transfer printing at 23 °C and 5 bar as shown in Figure 6a. In order to test the mechanical flexibility and robustness of the devices, bending tests were carried out. The SEM images in Figure 6a shows that cracks or fractures were not formed near the bonding region of ZnO NW and Au electrodes even after 10^3 cycles of bending. The current−voltage characteristics and response to UV illumination were measured after 10^3 cycles of bending, and no significant degradation caused by the damage or breakage of NW−electrode bonding could be observed. The flexible device exhibited excellent mechanical robustness and durability, which can be attributed to the mechanically strong bonding by embedding the ZnO NW into metal electrodes via the room-temperature compressive transfer printing method. We can conclude that the room-temperature compressive transfer printing allows a facile fabrication of mechanically robust nanoelectronic devices on flexible substrates.

In the present work, we have demonstrated the room-temperature compressive transfer printing technology on a single device with one pair of electrodes. However, this technology can be potentially applicable to a large-scale substrate with multiple devices. In the first transfer step (from the donor substrate to the intermediate substrate), the NWs can be aligned in parallel and transferred with a uniform density. Also, the number and location of NWs can be accurately controlled by using selective transfer on predefined regions (e.g., photoresist trenches defined by photolithography) during the first transfer process. Then, in the second transfer step (from the intermediate substrate to the target substrate), NWs with uniform density at well-defined locations on the intermediate substrate can be transferred and bonded onto the substrate with multiple devices. In this step, conventional optical methods can be used for the alignment between NWs and devices on a large area substrate. Since uniform pressure can be applied by air-pressurized rubber chamber throughout the entire substrate, high yield of NW transfer and bonding can be achieved.

CONCLUSION

In summary, we have demonstrated that NWs can be transferred and embedded into Au electrodes by room-temperature compressive transfer printing at low-pressure (5 bar) conditions. The submergence of NWs into the surface of electrode provides mechanically robust bonding. We have found that the electrical contact could be converted from a Schottky to Ohmic contact via a thermal annealing treatment at 250 °C due to the diffusion of Cr through the Au layer and formation of a direct contact with ZnO NW. The application of fabricated devices was successfully demonstrated as a UV sensor in ambient condition and as a hydrogen sensor. Furthermore, we have demonstrated that this process could be successfully applied for the fabrication of flexible NW-based electronic devices with mechanical flexibility and robustness. We believe that this method will be very useful for the fabrication of both large area and flexible NW-based electronic devices such as field effect transistors, light emitting diodes, and sensors with mechanically robust and electrically stable properties due to the advantages of moderate process conditions, low-cost, simple, and parallel manufacturing without complicated additional postprocessing steps for enhancing the mechanical and electrical contact properties.

ASSOCIATED CONTENT

Supporting Information

(1) Temperature profiles for the annealing process; (2) numerical analysis for the submergence of ZnO NW into Au electrodes and for the bonding strength between ZnO NW and Au electrodes; and (3) microscopic analysis of the Au-ZnO NW contact region and electrical measurement after thermal annealing treatment at 250 °C for 5 min. This material is available free of charge via the Internet at http://pubs.acs.org.

AUTHOR INFORMATION

Corresponding Author

*E-mail: inkyu@kaist.ac.kr (I.K.); jihyelee@kimm.re.kr (J.H.).

Notes

The authors declare no competing financial interest.

ACKNOWLEDGMENTS

This research was supported by the Future-based Technology Development Program (Nano Fields) (2012-0006201) and Basic Science Research Program (2012-0002021) through the National Research Foundation of Korea (NRF) and Global Frontier Project (Smart IT Convergence System Research Center; 2011-0031870) funded by the Korean government (MEST).

REFERENCES

(1) Yuan, Z.-Y.; Zhang, X.-B.; Su, B.-L. Moderate hydrothermal synthesis of potassium titanate nanowires. *Appl. Phys. A: Mater. Sci. Process.* **2004**, *78*, 1063−1066.

(2) Greene, L. E.; Law, M.; Goldberger, J.; Kim, F.; Johnson, J. C.; Zhang, Y.; Saykally, R. J.; Yang, P. Low-Temperature Wafer-Scale Production of ZnO Nanowire Arrays. *Angew. Chem., Int. Ed.* **2003**, *42*, 3031−3034.

(3) Li, Y.; Wang, J.; Deng, Z.; Wu, Y.; Sun, X.; Yu, D.; Yang, P. Bismuth Nanotubes: A Rational Low-Temperature Synthetic Route. *J. Am. Chem. Soc.* **2001**, *123*, 9904−9905.

(4) Chen, C.-C.; Yeh, C.-C. Large-Scale Catalytic Synthesis of Crystalline Gallium Nitride Nanowires. *Adv. Mater.* **2000**, *12*, 738−741.

(5) Kim, J.; Li, Z.; Park, I. Direct synthesis and integration of functional nanostructures in microfluidic devices. *Lab Chip* **2011**, *11*, 1946−1951.

(6) Bao, J.; Zimmler, M. A.; Capasso, F. Broadband ZnO Single-Nanowire Light-Emitting Diode. *Nano Lett.* **2006**, *6*, 1719−1722.

(7) Wan, Q.; Li, Q. H.; Chen, Y. J.; Wang, T. H.; He, X. L.; Li, J. P.; Lin, C. L. Fabrication and ethanol sensing characteristics of ZnO nanowire gas sensors. *Appl. Phys. Lett.* **2004**, *84*, 3654.

(8) Lim, M. A.; Kim, D. H.; Park, C. O.; Lee, Y. W.; Han, S. W.; Li, Z.; Williams, R. S.; Park, I. A New Route toward Ultrasensitive, Flexible Chemical Sensors: Metal Nanotubes by Wet-Chemical Synthesis along Sacrificial Nanowire Templates. *ACS Nano* **2011**, *6*, 598−608.

(9) Yeh, P.-H.; Li, Z.; Wang, Z. L. Schottky-Gated Probe-Free ZnO Nanowire Biosensor. *Adv. Mater.* **2009**, *21*, 4975−4978.

(10) Lim, M. A.; Lee, Y. W.; Han, S. W.; Park, I. Novel fabrication method of diverse one-dimensional Pt/ZnO hybrid nanostructures and its sensor application. *Nanotechnology* **2010**, *22*, 035601.

(11) Cui, Y.; Zhong, Z.; Wang, D.; Wang, W. U.; Lieber, C. M. High Performance Silicon Nanowire Field Effect Transistors. *Nano Lett.* **2003**, *3*, 149−152.

(12) Ko, S. H.; Park, I.; Pan, H.; Misra, N.; Rogers, M. S.; Grigoropoulos, C. P.; Pisano, A. P. ZnO nanowire network transistor fabrication on a polymer substrate by low-temperature, all-inorganic nanoparticle solution process. *Appl. Phys. Lett.* **2008**, *92*, 154102.

(13) Kim, J.; Hong, J. W.; Kim, D. P.; Shin, J. H.; Park, I. Nanowire-integrated microfluidic devices for facile and reagent-free mechanical cell lysis. *Lab Chip* **2012**, *12*, 2914−2921.
(14) Yang, R.; Qin, Y.; Dai, L.; Wang, Z. L. Power generation with laterally packaged piezoelectric fine wires. *Nat. Nanotechnol.* **2009**, *4*, 34−39.
(15) Lee, Y. W.; Lim, M. A.; Kang, S. W.; Park, I.; Han, S. W. Facile synthesis of noble metal nanotubes by using ZnO nanowires as sacrificial scaffolds and their electrocatalytic properties. *Chem. Commun.* **2011**, *47*, 6299−6301.
(16) Suehiro, J.; Nakagawa, N.; Hidaka, S.-I.; Ueda, M.; Imasaka, K.; Higashihata, M.; Okada, T.; Hara, M. Dielectrophoretic fabrication and characterization of a ZnO nanowire-based UV photosensor. *Nanotechnology* **2006**, *17*, 2567−2573.
(17) Wang, D.; Zhu, R.; Zhou, Z.; Ye, X. Contact Behaviors Between Zinc Oxide Nanowires and Metal Electrodes. *J. Nanosci. Nanotechnol.* **2009**, *9*, 862−865.
(18) Ingole, S.; Aella, P.; Hearne, S. J.; Picraux, S. T. Directed assembly of nanowire contacts using electrodeposition. *Appl. Phys. Lett.* **2007**, *91*, 033106.
(19) Suh, D.-I.; Lee, S.-Y.; Hyung, J.-H.; Kim, T.-H.; Lee, S.-K. Multiple ZnO Nanowires Field-Effect Transistors. *J. Phys. Chem. C* **2008**, *112*, 1276−1281.
(20) Li, X.; Chin, E.; Sun, H.; Kurup, P.; Gu, Z. Fabrication and integration of metal oxide nanowire sensors using dielectrophoretic assembly and improved post-assembly processing. *Sens. Actuators, B* **2010**, *148*, 404−412.
(21) Chang, Y.-K.; Hong, F. C.-N. The fabrication of ZnO nanowire field-effect transistors combining dielectrophoresis and hot-pressing. *Nanotechnology* **2009**, *20*, 235202.
(22) Ye, H.; Gu, Z.; Yu, T.; Gracias, D. H. Integrating Nanowires With Substrates Using Directed Assembly and Nanoscale Soldering. *IEEE Trans. Nanotechnol.* **2006**, *5*, 62−66.
(23) Li, Q.; Koo, S.-M.; Richter, C. A.; Edelstein, M. D.; Bonevich, J. E.; Kopanski, J. J.; Suehle, J. S.; Vogel, E. M. Precise Alignment of Single Nanowires and Fabrication of Nanoelectromechanical Switch and Other Test Structures. *IEEE Trans. Nanotechnol.* **2007**, *6*, 256−262.
(24) Fan, Z.; Ho, J. C.; Jacobson, Z. A.; Yerushalmi, R.; Alley, R. L.; Razavi, H.; Javey, A. Wafer-Scale Assembly of Highly Ordered Semiconductor Nanowire Arrays by Contact Printing. *Nano Lett.* **2008**, *8*, 20−25.
(25) Hangarter, C. M.; Bangar, M.; Hernandez, S. C.; Chen, W.; Deshusses, M. A.; Mulchandani, A.; Myung, N. V. Maskless electrodeposited contact for conducting polymer nanowires. *Appl. Phys. Lett.* **2008**, *92*, 073104.
(26) Lee, W. S.; Won, S. J.; Park, J. H.; Lee, J. H.; Park, I. Thermo-compressive transfer printing for facile alignment and robust device integration of nanowires. *Nanoscale* **2012**, *4*, 3444−3449.
(27) Brillson, L. J.; Lu, Y. ZnO Schottky barriers and Ohmic contacts. *J. Appl. Phys.* **2011**, *109*, 121301.
(28) Benjamin, J. S.; Volin, T. E. The mechanism of mechanical alloying. *Metall. Mater. Trans. B* **1974**, *5*, 1929−1934.
(29) Lu, Y.; Huang, J. Y.; Wang, C.; Sun, S.; Lou, J. Cold welding of ultrathin gold nanowires. *Nat. Nanotechnol.* **2010**, *5*, 218−224.
(30) Garnett, E. C.; Cai, W.; Cha, J. J.; Mahmood, F.; Connor, S. T.; Christoforo, M. G.; Cui, Y.; McGehee, M. D.; Brongersma, M. L. Self-limited plasmonic welding of silver nanowire junctions. *Nat. Mater.* **2012**, *11*, 241−249.
(31) Higashino, T.; Suga, T.Finite Element Analysis of the Effect of Surface Roughness on Nanometer-scale Contact. In *Proceedings of the 6th International Conference on Polymers Adhesives Microelectronics Photonics*; Tokyo, Japan2007; pp 209−212
(32) Kim, Y.-J.; Son, K.; Choi, I.-C.; Choi, I.-S.; Park, W. I.; Jang, J.-I. Exploring Nanomechanical Behavior of Silicon Nanowires: AFM Bending Versus Nanoindentation. *Adv. Funct. Mater.* **2011**, *21*, 279−286.
(33) Huang, Y.; Qiu, H.; Wang, F.; Pan, L.; Tian, Y.; Wu, P. Effect of annealing on the characteristics of Au/Cr bilayer films grown on glass. *Vacuum* **2003**, *71*, 523−528.
(34) Kuma, K.; Moriizumi, T.; Yasudo, T. Fabrication and properties of ZnO thin films by DC diode sputtering technique using Zn target. *J. Inst. Electr. Eng. Jpn.* **1976**, *96*, 389−396.
(35) Lupan, Q.; Chai, G.; Chow, L.; Emelchenko, G. A.; Heinrich, H.; Ursaki, V. V.; Gruzintsev, A. N.; Tiginyanu, I. M.; Redkin, A. N. Ultraviolet photoconductive sensor based on single ZnO nanowire. *Phys. Status Solidi A* **2010**, *207*, 1735−1740.
(36) Hu, Y.; Zhou, J.; Yeh, P.-H.; Li, Z.; Wei, T.-Y.; Wang, Z. L. Supersensitive, Fast-Response Nanowire Sensors by Using Schottky Contacts. *Adv. Mater.* **2010**, *22*, 3327−3332.
(37) Lupan, O.; Chai, G.; Chow, L. Novel hydrogen gas sensor based on single ZnO nanorod. *Microelectron. Eng.* **2008**, *85*, 2220−2225.